Controllable tuning of exciton polariton condensate flow in a waveguide by phase modulation

Qiang Ai,[1,*] Peilin Wang,[2,*] Xiaokun Zhai,[1] Chunzi Xing,[1] Xinmiao Yang,[1] Zaharias Hatzopoulos,[3] Pavlos G. Savvidis,[4,5] Tianyu Liu,[1] Yong Zhang,[2,†] Stefan Schumacher,[6,7,8] Xuekai Ma,[6] and Tingge Gao[1,‡]

[1]*Department of Physics, School of Science, Tianjin University, Tianjin 300072, China*

[2]*Center for Applied Mathematics and KL-AAGDM, Tianjin University, Tianjin 300072, China*

[3]*Institute of Electronic Structure and Laser (IESL), Foundation for Research and Technology-Hellas (FORTH), 71110 Heraklion, Greece*

[4]*Key Laboratory for Quantum Materials of Zhejiang Province, Department of Physics, Westlake University, Hangzhou, Zhejiang 310024, China*

[5]*Department of Physics, School of Science, Westlake University, Hangzhou 310014, China*

[6]*Department of Physics and Center for Optoelectronics and Photonics Paderborn (CeOPP), Paderborn University, Warburger Strasse 100, 33098 Paderborn, Germany*

[7]*Institute for Photonic Quantum Systems (PhoQS), Paderborn University, 33098 Paderborn, Germany*

[8]*Wyant College of Optical Sciences, University of Arizona, Tucson, Arizona 85721, USA*

(Received 18 April 2025; revised 1 August 2025; accepted 8 September 2025; published 10 October 2025)

Controllable particle flows play an important role in modern optics and photonics. Switching off photon flows using optical methods is challenging to realize due to the limited ways to control photon interactions. Here, we realize an exciton polariton condensate flow in a waveguide of a GaAs microcavity with a potential gradient by using a tight pumping spot. Polariton condensate flow along the waveguide can be periodically switched off and on globally by adding a second local small spot on the waveguide. Tuning the pumping density or position induces a pump intensity and position-dependent potential barrier modulating the phase of the condensate by a polariton-exciton interaction. This enables us to study the polariton condensation process in a waveguide by phase modulation, which could find important applications in integrated photonic circuits and chips.

DOI: 10.1103/gyjg-46hv

I. INTRODUCTION

Modulating photon flow attracts significant attention because of the important role it plays in integrated photonic circuits and chips [1–5]. Recently, controlling photon propagation is realized in PT-symmetric photonic systems near the exceptional point [6–11]. In addition, unidirectional photon transport is shown in topological systems [12,13]. In these photonic structures, photon flow can be modulated and routed along particular directions by engineering specific structure parameters, for example, gain and loss coefficients or the coupling strength between the nearest lattice sites [14–18]. However, optically controlling photon flow, for example, the photon propagation being switched off and on along a waveguide using a purely optical control knob, is not easy to be realized due to the limited tunability of the interaction between photons.

Exciton polaritons are hybrid light-matter quasiparticles, created due to the strong coupling between an exciton and a photon mode [19,20]. In microcavities, exciton polariton Bose-Einstein condensation has been realized through stimulated scattering at much higher temperatures than cold atom condensates [21–24]. Importantly, such exciton polariton condensates can be efficiently controlled by optical means [25–32]. For example, polaritons can be switched off in a four-wave mixing experiment which relies on the resonant injection of degenerate polaritons [33]. Switching off the polariton condensate can also be realized in coupled potential traps near an exceptional point [34]. In waveguide structures, optical and electrical schemes have been employed to control the flow of exciton polaritons [35–39]. Its implementation typically hinges on the precise manipulation of the condensate phase or gating, for example, by utilizing a potential barrier formed by an exciton reservoir [40], or by resonant polaritons [41]. However, the above works route or control only part of the polaritons, and they cannot switch off the entire polariton condensate along the waveguide. To entirely switch off the polariton condensate flow in the photonic waveguide, phase modulation with a different pumping configuration is needed.

In this work we realize a method to repeatedly (in a periodic fashion) switch off and on an extended polariton condensate flow across a one-dimensional waveguide. The waveguide has a small potential gradient in the range of 200 μm, and we use two lasers with the same wavelength. The first laser nonresonantly excites the polariton condensate flow which propagates along the one-dimensional (1D) waveguide, and the second laser injects an exciton reservoir at another position which modulates the phase of the condensate, leading to periodic on and off switching of the entire polariton condensate flow. Our work allows to investigate polariton condensate flow manipulation using direct optical means, which

*These authors contributed equally to this work.
†Contact author: zhang_yong@tju.edu.cn
‡Contact author: tinggegao@tju.edu.cn

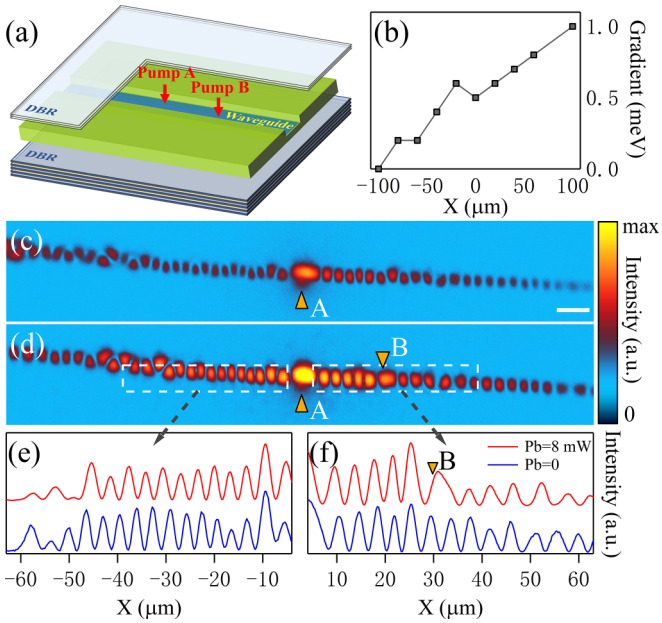

FIG. 1. Schematic graph of the waveguide within a microcavity and the condensation phase modulation induced by the second pump spot. (a) Schematic graph of a waveguide with a potential gradient. (b) The gradient variation of the waveguide. (c) Real-space images when only spot A excites the waveguide. (d) Real-space images when spots B and A excite the waveguide. The distance between spots A and B is 30 μm. (e), (f) The line profile of the mode shift on the (e) left and (f) right side of pump spot A. The dashed boxes indicate the selected area. Scale bars: 10 μm.

can find future applications in polariton integrated chips and circuits.

II. THE GENERATION OF EXCITON POLARITON CONDENSATE FLOW

We use a GaAs microcavity whose details can be found in Ref. [34]. The microcavity is cooled in a cryostat at 6 K. A waveguide with a width of around 5 μm and length of around 200 μm is formed unintentionally during the growth process [Fig. 1(a)]. A potential gradient exists along the waveguide due to the wedge design of the microcavity length. We measure the energy of the polariton modes below threshold along the waveguide, which shows the potential gradient is around 5×10^{-3} meV/μm [Fig. 1(b)]. We split the cw pumping laser whose wavelength is tuned to be around 760 nm into two beams with a mechanical chopper (duty cycle: 5%) to reduce the heating effect. The first arm excites the waveguide with a pumping density of around 90 mW, which is around $1.2P_{\text{th}}$ [the condensation process is shown in the Supplemental Material (SM) [42]].

Generally, a polariton interference pattern can only appear when a tight pumping spot excites the waveguide area close to the end. In our experiment, although pumping spot A is in the middle position of the waveguide, polaritons can propagate to the two waveguide ends and are reflected backwards, owing to the high quality of the microcavity. The reflected polaritons interfere with the propagating polaritons, thus we observe a periodic interference pattern along the waveguide. We note that a bright emission lobe exists at the center of spot A, which is due to the high energy of the polaritons which are not confined between the energy barrier that results from the local blueshift of pump spot A and the two waveguide ends, as shown in the measured dispersion in SM [42]. This kind of periodic polariton mode does not depend on the position of pump spot A and can be reproduced almost anywhere along the waveguide.

The polariton mode distribution is affected by the disorder potentials or the inhomogeneity within the 1D waveguide. In this case, the polariton intensity distribution or the lobe size is not uniform. We measured the disorder potential distribution using a large Gaussian spot with a width of around 40 μm to excite the waveguide below threshold, where the eigenmodes of the waveguide are shown in SM [42]. These random distributed disorder potentials are not consistent with the periodic polariton interference pattern shown in Fig. 1(c).

III. THE PATTERN DISTRIBUTION OF PERIODIC POLARITON MODE

The above polariton condensate flow along the waveguide can be tuned by introducing a nonresonant tight pumping spot B which can modulate the propagating polariton phase. The phase difference of the polaritons across the energy barrier of this second spot can be calculated by the formula [40]

$$\delta\varphi = L\left(\frac{\sqrt{2mE_k}}{\hbar} - \frac{\sqrt{2m(E_k - V)}}{\hbar}\right). \tag{1}$$

In our case E_k is the kinetic energy of the polaritons, $V = V_0 + kx$ is the potential barrier created by spot B where V_0 is the potential due to the exciton reservoir, k is the coefficient of the potential gradient, x is the distance between the two spots, and L is the width of the local potential barrier. In Ref. [40], the local control beam induces phase modulation for one arm, which thus affects the routing of the polariton condensate. In our experiment, the injected polariton condensate transports back and forth across the entire waveguide, where the second pumping spot can induce the phase modulation nonlocally, thus the emission intensity along the waveguide becomes more sensitive to the appearance of the second spot.

Experimentally, pumping spot B is excited by a distance of 30 μm away from spot A and a pumping density of 8 mW ($0.11P_{\text{th}}$). With the appearance of spot B, we find the polariton interference pattern is tuned. The bright emission lobes at the left and right side of pump spot A become dark and vice versa [from Fig. 1(c) to Fig. 1(d)]; more clear data of the intensity mode shift and phase modulation are shown in the line profile plotted in Fig. 1(e) (left side of pumping spot A) and Fig. 1(f) (right side of pumping spot A). This kind of polariton mode tuning confirms the phase modulation results from the tunneling through a potential barrier formed by the injected local exciton reservoir from spot B. We note that the phase modulation is not uniform across the waveguide, which is due to the random disorder or inhomogeneity of the waveguide. By further increasing the pumping density of spot B to be $0.22P_{\text{th}}$, which tunes the phase of the polariton condensate such that destructive interference occurs across the waveguide, the emission intensity is decreased to be around

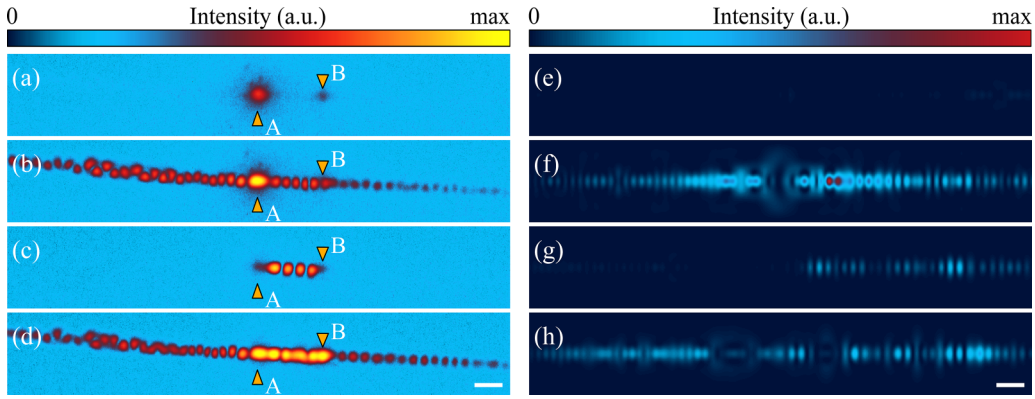

FIG. 2. Polariton condensation is switched off and on under different pumping densities of spot B. (a)–(d) Real-space images of polariton condensation with different pumping densities of pump spot B ($0.22P_{\text{th}}$, $0.42P_{\text{th}}$, $0.63P_{\text{th}}$, and $0.75P_{\text{th}}$, respectively), The distance between the two pump spots is fixed at approximately 30 μm. (e)–(h) Theoretical intensity distribution along the waveguide with different pumping densities of spot B. Scale bars: 10 μm.

8.8% [Fig. 2(a)]. Compared with Ref. [40] which tunes the phase of one arm with another arm being unchanged, our results realize the modulation of the polaritons which propagate along the entire waveguide, such that the emission intensity is switched off by the second local spot.

IV. PERIODIC TUNING OF POLARITON PATTERNS INDUCED BY THE SECOND PUMP

More importantly, the above polariton pattern depends periodically on the pumping density of spot B. In Figs. 2(a)–2(d) we plot the real-space images of the waveguide as a function of the pumping densities of spot B (from $0.22P_{\text{th}}$ to $0.75P_{\text{th}}$). Figure 2(b) clearly shows the polariton modes across the waveguide appear again under a pumping density of $0.42P_{\text{th}}$ with the same energy, plotted in the SM [42]. Under a higher pumping density of spot B ($0.63P_{\text{th}}$), the polariton condensate across the waveguide disappears and a standing-wave pattern is observed between pumping spots A and B [Fig. 2(c)]. We note that the bright emission lobe at the center of pumping spot A becomes invisible when the polariton standing-wave pattern appears with an energy smaller than the polaritons distributed along the waveguide (the dispersion is shown in SM [42]), indicating a potential barrier is built up between spots A and B. Under a pumping density of around $0.75P_{\text{th}}$ of spot B, a polariton condensate along the waveguide is formed again and the standing-wave pattern becomes more pronounced [shown in Fig. 2(d)].

We simulate the above experimental results using a Gross-Pitaevskii (GP) equation. To simplify the discussion, a two-dimensional (2D) model is used which describes the polariton distribution along a straight waveguide. In dimensionless form the model reads

$$\begin{aligned} \mathrm{i}\frac{\partial \psi}{\partial t} &= \left[-\frac{1}{2}\Delta + V(x,y) + g_c|\psi|^2 \right. \\ &\quad \left. + \frac{\mathrm{i}}{2}(Rn - \gamma_c) + g_r n\right]\psi \\ \frac{\partial n}{\partial t} &= -(\gamma_r + R|\psi|^2)n + P(x,y), \end{aligned} \tag{2}$$

where $\psi := \psi(x, y, t)$ is the wave function of the polariton condensate, $n := n(x, y, t)$ represents the excitation reservoir density, $V(x, y)$ is the external potential, $P(x, y)$ is the pump density, and x and y are the spatial coordinates along the waveguide. Details of the simulations are discussed in the SM [42] (which includes Refs. [43,44]). The simulated intensity distribution along the waveguide is shown in Figs. 2(e)–2(h). When the pumping density of spot B increases to $0.20P_{\text{th}}$, the density of polaritons along the waveguide can be neglected, as shown in Fig. 2(e). The polariton density increases along the waveguide with a further enhancement of the pumping density of spot B at $0.40P_{\text{th}}$ [Fig. 2(f)]. Under a pumping density of spot B of $0.60P_{\text{th}}$, a standing-wave mode appears between the two spots. The emission intensity on the left side of spot A [Fig. 2(g)], which corresponds to the part of the polariton condensate extending across the waveguide, is greatly reduced. Lastly, the polariton condensate extending across the waveguide appears again under the largest pumping density of spot B at $0.88P_{\text{th}}$ [Fig. 2(h)]. The simulated intensity along the waveguide agrees very well with the experimental results (there exists some difference between the pumping densities of spot B with experiments, which is due to the fact that the waveguide is not perfectly straight, and the width of the waveguide is not constant). The 2D simulation model can give the same mode distribution of the polariton modes, for example, the lobe number and intensity.

The relative distance between spot B and spot A can also create a periodic switching of the polariton condensate along the waveguide. Figures 3(a)–3(c) show the periodic dependence of the real-space images of the polariton condensate along the waveguide when the position of pumping spot B (the pumping density of spot B is constant, around $0.5P_{\text{th}}$) is farther away from spot A. Under a certain distance between the two spots, the polariton condensate disappears along the waveguide where the position-dependent potential barrier $V = V_0 + kx$ created by spot B leads to destructive interference. A theoretical simulation can reproduce experimental results perfectly, as plotted in Figs. 3(d)–3(f).

In addition, the sign of the potential gradient along the waveguide affects the above phase modulation depending on the appearance of the second pumping spot. In the experiment,

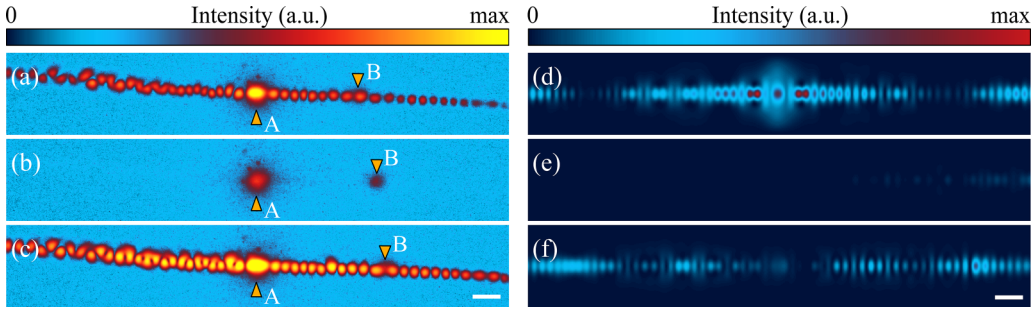

FIG. 3. Polariton condensation is switched off and on by changing the position of spot B. (a)–(c) Real-space images of polariton condensation with different positions of pumping spot B. The pumping density of spot B is constant, around $0.5P_{\text{th}}$, and the distances between two pump spots are 37, 44, and 47 μm, respectively. (d)–(f) Theoretical intensity distribution along the waveguide by changing the position of spot B. Scale bars: 10 μm.

we place another tight pumping spot C below threshold on the left side of spot A. First, we fix the relative distance between spots A and C to be 34 μm, and the pumping densities of spots A and C to be around $1.2P_{\text{th}}$ and $0.58P_{\text{th}}$, respectively [Fig. 4(a)], where the condensate flow can be switched on. Second, the polariton condensate flow along the waveguide is switched off when the pumping density of spot C is increased to $0.6P_{\text{th}}$. Due to the smaller position-dependent potential kx at the left side of spot A, a higher exciton reservoir potential V_0 is needed to tune the phase of the polariton condensate. In this case, a higher pumping density of spot C has to be kept [in the experiment the pumping density of spot C is needed to be tuned to $0.60P_{\text{th}}$, which is much larger than $0.22P_{\text{th}}$ of spot B in Fig. 2(a)], and the potential barrier due to the local blueshift of the exciton reservoir of spot C can sustain the polariton standing-wave mode between the two spots. Thus we can observe a polariton condensate along the waveguide being switched off with the appearance of a standing-wave

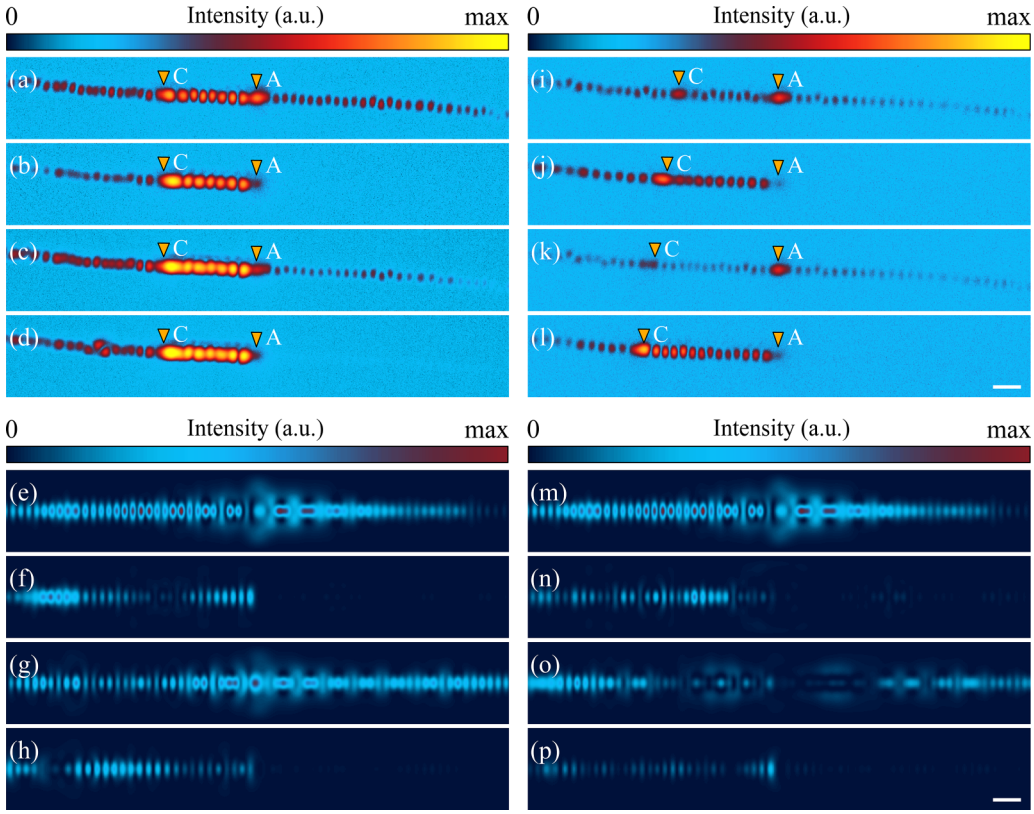

FIG. 4. Polariton condensation is switched off and on with different pumping configurations of spot C. (a)–(d) Real-space images of polariton condensation with different pumping densities of pump C ($0.51P_{\text{th}}$, $0.60P_{\text{th}}$, $0.74P_{\text{th}}$, and $0.90P_{\text{th}}$, respectively), The distance between the two pump spots is fixed at approximately 34 μm. (i)–(l) Real-space images of polariton condensation with different positions of pumping spot C. The pumping density of spot C is constant, around $0.6P_{\text{th}}$, and the distances between the two pump spots are 35, 40, 44, and 48 μm, respectively. (e)–(h) Theoretical intensity distribution along the waveguide with different pumping densities of spot C. (m)–(p) Theoretical intensity distribution by changing the position of spot C. Scale bars: 10 μm.

pattern at the same time directly, as shown in Fig. 4(b). This is different from Fig. 2(a). Further increasing the pumping density of spot C leads to the periodic on and off switching of the polariton condensate across the waveguide, with a higher population of the polariton standing mode between the two spots [Figs. 4(c) and 4(d)]. Similarly as the case between spots A and B, a polariton condensate across the waveguide can also be periodically switched off and on when the position of spot B is varied along the waveguide, as plotted in Figs. 4(i)–4(l) with a standing-wave mode built between the two spots. The above experimental results can be reproduced perfectly by the theoretical simulation, as shown in Figs. 4(e)–4(h) and Figs. 4(m)–4(p).

On the contrary, the polariton emission intensity modulation by the second tight spot will disappear when pumping laser A is replaced by a large Gaussian spot above the threshold where the polariton condensate created is trapped in the disorder potential of the waveguide, as shown in SM [42]. In this case, the second spot cannot tune the phase of the trapped polariton condensate and the emission intensity of the waveguide always increases. This confirms the role of the phase modulation to switch off the polariton condensate across the waveguide.

V. CONCLUSION

To conclude, our work realizes the periodic off and on switching of a polariton condensate across a waveguide using two tightly focused pumping spots, inducing a phase modulation through polariton-exciton interactions. The simulation using the GP equations agrees well with the experimental results. Our work shows how to control the polariton condensate using a simple optical method and can find applications in optoelectronic circuits based on exciton polariton condensates.

ACKNOWLEDGMENTS

T.G. acknowledges the support from the National Natural Science Foundation of China (NSFC, No. 12174285 and No. 12474315). X.Z. acknowledges support from the National Natural Science Foundation of China (NSFC, No. 12504372) and the China Postdoctoral Science Foundation - Tianjin Joint Support Program under Grant (No. 2025T003TJ). This work is also partially supported by the National Key R&D Program of China No. 2024YFA1012803, basic research fund of Tianjin University under Grant No. 2025XJ21-0010, and the National Natural Science Foundation of China No. 12271400 (P.W. and Y.Z.). P.G.S. acknowledges financial support from the Innovation Program for Quantum Science and Technology (Grant No. 2023ZD0300300) and the Westlake University project (No. 102510036022301).

DATA AVAILABILITY

The data that support the findings of this article are not publicly available. The data are available from the authors upon reasonable request.

[1] K. Fang, Z. Yu, and S. Fan, Realizing effective magnetic field for photons by controlling the phase of dynamic modulation, Nat. Photonics **6**, 782 (2012).

[2] D.-W. Wang, H.-T. Zhou, M.-J. Guo, J.-X. Zhang, J. Evers, and S.-Y. Zhu, Optical diode made from a moving photonic crystal, Phys. Rev. Lett. **110**, 093901 (2013).

[3] J. D. Joannopoulos, P. R. Villeneuve, and S. Fan, Photonic crystals: Putting a new twist on light, Nature (London) **386**, 143 (1997).

[4] T. Zhu, C. Guo, J. Huang, H. Wang, M. Orenstein, Z. Ruan, and S. Fan, Topological optical differentiator, Nat. Commun. **12**, 680 (2021).

[5] S. G. Johnson, S. Fan, P. R. Villeneuve, J. D. Joannopoulos, and L. A. Kolodziejski, Guided modes in photonic crystal slabs, Phys. Rev. B **60**, 5751 (1999).

[6] V. V. Konotop, J. Yang, and D. A. Zezyulin, Nonlinear waves in $\mathcal{PT}$-symmetric systems, Rev. Mod. Phys. **88**, 035002 (2016).

[7] C. M. Bender and S. Boettcher, Real spectra in non-Hermitian Hamiltonians having $\mathcal{PT}$ symmetry, Phys. Rev. Lett. **80**, 5243 (1998).

[8] B. Peng, Ş. K. Özdemir, F. Lei, F. Monifi, M. Gianfreda, G. L. Long, S. Fan, F. Nori, C. M. Bender, and L. Yang, Parity–time-symmetric whispering-gallery microcavities, Nat. Phys. **10**, 394 (2014).

[9] L. Feng, Y.-L. Xu, W. S. Fegadolli, M.-H. Lu, J. E. Oliveira, V. R. Almeida, Y.-F. Chen, and A. Scherer, Experimental demonstration of a unidirectional reflectionless parity-time metamaterial at optical frequencies, Nat. Mater. **12**, 108 (2013).

[10] L. Chang, X. Jiang, S. Hua, C. Yang, J. Wen, L. Jiang, G. Li, G. Wang, and M. Xiao, Parity–time symmetry and variable optical isolation in active–passive-coupled microresonators, Nat. Photon. **8**, 524 (2014).

[11] N. Moiseyev, *Non-Hermitian Quantum Mechanics* (Cambridge University Press, Cambridge, U.K., 2011).

[12] L. Wang, L. Yuan, X. Chen, and S. Fan, Single-photon transport in a topological waveguide from a dynamically modulated photonic system, Phys. Rev. Appl. **14**, 014063 (2020).

[13] Y. Yang, X. Qian, L. Shi, X. Shen, and Z. H. Hang, Unidirectional transport in amorphous topological photonic crystals, Sci. China Phys. Mech. Astron. **66**, 274212 (2023).

[14] K.-H. O and K.-H. Kim, Parity-time phase transition of topological corner states in square lattice photonic crystal structures, Adv. Photonics Res. **4**, 2200087 (2023).

[15] H. Zhou, J. Y. Lee, S. Liu, and B. Zhen, Exceptional surfaces in *PT*-symmetric non-Hermitian photonic systems, Optica **6**, 190 (2019).

[16] K. Ding, Z. Q. Zhang, and C. T. Chan, Coalescence of exceptional points and phase diagrams for one-dimensional $\mathcal{PT}$-symmetric photonic crystals, Phys. Rev. B **92**, 235310 (2015).

[17] X. Ni, D. Smirnova, A. Poddubny, D. Leykam, Y. Chong, and A. B. Khanikaev, $\mathcal{PT}$ phase transitions of edge states at $\mathcal{PT}$ symmetric interfaces in non-Hermitian topological insulators, Phys. Rev. B **98**, 165129 (2018).

[18] S. Weimann, M. Kremer, Y. Plotnik, Y. Lumer, S. Nolte, K. G. Makris, M. Segev, M. C. Rechtsman, and A. Szameit, Topologically protected bound states in photonic parity–time-symmetric crystals, Nat. Mater. **16**, 433 (2017).

[19] C. Weisbuch, M. Nishioka, A. Ishikawa, and Y. Arakawa, Observation of the coupled exciton-photon mode splitting in a semiconductor quantum microcavity, Phys. Rev. Lett. **69**, 3314 (1992).

[20] A. Kavokin, J. J. Baumberg, G. Malpuech, and F. P. Laussy, *Microcavities* (Oxford University Press, Oxford, U.K., 2017).

[21] J. Kasprzak, M. Richard, S. Kundermann, A. Baas, P. Jeambrun, J. M. J. Keeling, F. Marchetti, M. Szymańska, R. André, V. Savona, P. B. Littlewood, B. Deveaud, and L. S. Dang, Bose–Einstein condensation of exciton polaritons, Nature (London) **443**, 409 (2006).

[22] R. Balili, V. Hartwell, D. Snoke, L. Pfeiffer, and K. West, Bose-Einstein condensation of microcavity polaritons in a trap, Science **316**, 1007 (2007).

[23] T. Byrnes, N. Y. Kim, and Y. Yamamoto, Exciton–polariton condensates, Nat. Phys. **10**, 803 (2014).

[24] V. Ardizzone, F. Riminucci, S. Zanotti, A. Gianfrate, M. Efthymiou-Tsironi, D. Suàrez-Forero, F. Todisco, M. De Giorgi, D. Trypogeorgos, G. Gigli, K. Baldwin, L. Pfeiffer, D. Ballarini, H. S. Nguyen, D. Gerace, and D. Sanvitto, Polariton Bose–Einstein condensate from a bound state in the continuum, Nature (London) **605**, 447 (2022).

[25] T. Gao, E. Estrecho, K. Bliokh, T. Liew, M. Fraser, S. Brodbeck, M. Kamp, C. Schneider, S. Höfling, Y. Yamamoto, F. Nori, Y. Kivshar, A. Truscott, R. Dall, and E. Ostrovskaya, Observation of non-Hermitian degeneracies in a chaotic exciton-polariton billiard, Nature (London) **526**, 554 (2015).

[26] T. Gao, G. Li, E. Estrecho, T. C. H. Liew, D. Comber-Todd, A. Nalitov, M. Steger, K. West, L. Pfeiffer, D. W. Snoke, A. V. Kavokin, A. G. Truscott, and E. A. Ostrovskaya, Chiral modes at exceptional points in exciton-polariton quantum fluids, Phys. Rev. Lett. **120**, 065301 (2018).

[27] X. Ma, B. Berger, M. Aßmann, R. Driben, T. Meier, C. Schneider, S. Höfling, and S. Schumacher, Realization of all-optical vortex switching in exciton-polariton condensates, Nat. Commun. **11**, 897 (2020).

[28] D. Sanvitto, F. M. Marchetti, M. Szymańska, G. Tosi, M. Baudisch, F. P. Laussy, D. Krizhanovskii, M. Skolnick, L. Marrucci, A. Lemaître, J. Bloch, C. Tejedor, and L. Viña, Persistent currents and quantized vortices in a polariton superfluid, Nat. Phys. **6**, 527 (2010).

[29] Y. del Valle-Inclan Redondo, C. Schneider, S. Klembt, S. Höfling, S. Tarucha, and M. D. Fraser, Optically driven rotation of exciton–polariton condensates, Nano Lett. **23**, 4564 (2023).

[30] I. Gnusov, S. Harrison, S. Alyatkin, K. Sitnik, J. Töpfer, H. Sigurdsson, and P. Lagoudakis, Quantum vortex formation in the "rotating bucket" experiment with polariton condensates, Sci. Adv. **9**, eadd1299 (2023).

[31] D. Ballarini, M. De Giorgi, E. Cancellieri, R. Houdré, E. Giacobino, R. Cingolani, A. Bramati, G. Gigli, and D. Sanvitto, All-optical polariton transistor, Nat. Commun. **4**, 1778 (2013).

[32] M. De Giorgi, D. Ballarini, E. Cancellieri, F. M. Marchetti, M. H. Szymanska, C. Tejedor, R. Cingolani, E. Giacobino, A. Bramati, G. Gigli, and D. Sanvitto, Control and ultrafast dynamics of a two-fluid polariton switch, Phys. Rev. Lett. **109**, 266407 (2012).

[33] F. Chen, H. Li, H. Zhou, S. Luo, Z. Sun, Z. Ye, F. Sun, J. Wang, Y. Zheng, X. Chen, H. Xu, H. Xu, T. Byrnes, Z. Chen, and J. Wu, Optically controlled femtosecond polariton switch at room temperature, Phys. Rev. Lett. **129**, 057402 (2022).

[34] Y. Li, X. Ma, Z. Hatzopoulos, P. G. Savvidis, S. Schumacher, and T. Gao, Switching off a microcavity polariton condensate near the exceptional point, ACS Photonics **9**, 2079 (2022).

[35] H. S. Nguyen, D. Vishnevsky, C. Sturm, D. Tanese, D. Solnyshkov, E. Galopin, A. Lemaître, I. Sagnes, A. Amo, G. Malpuech, and J. Bloch, Realization of a double-barrier resonant tunneling diode for cavity polaritons, Phys. Rev. Lett. **110**, 236601 (2013).

[36] F. Marsault, H. S. Nguyen, D. Tanese, A. Lemaître, E. Galopin, I. Sagnes, A. Amo, and J. Bloch, Realization of an all optical exciton-polariton router, Appl. Phys. Lett. **107**, 201115 (2015).

[37] V. Goblot, H. S. Nguyen, I. Carusotto, E. Galopin, A. Lemaître, I. Sagnes, A. Amo, and J. Bloch, Phase-controlled bistability of a dark soliton train in a polariton fluid, Phys. Rev. Lett. **117**, 217401 (2016).

[38] D. Liran, I. Rosenberg, K. West, L. Pfeiffer, and R. Rapaport, Fully guided electrically controlled exciton polaritons, ACS Photonics **5**, 4249 (2018).

[39] D. Suárez-Forero, F. Riminucci, V. Ardizzone, M. De Giorgi, L. Dominici, F. Todisco, G. Lerario, L. Pfeiffer, G. Gigli, D. Ballarini *et al.*, Electrically controlled waveguide polariton laser, Optica **7**, 1579 (2020).

[40] C. Sturm, D. Tanese, H. S. Nguyen, H. Flayac, E. Galopin, A. Lemaître, I. Sagnes, D. Solnyshkov, A. Amo, G. Malpuech, and J. Bloch, All-optical phase modulation in a cavity-polariton Mach–Zehnder interferometer, Nat. Commun. **5**, 3278 (2014).

[41] S. W. Lee, J. S. Lee, W. H. Choi, D. Choi, and S.-H. Gong, Ultra-compact exciton polariton modulator based on van der Waals semiconductors, Nat. Commun. **15**, 2331 (2024).

[42] See Supplemental Material at http://link.aps.org/supplemental/10.1103/gyjg-46hv for the condensation process of the exciton polariton; the waveguide fluorescence pumped by the large Gaussian spot pumping; the dispersion when the pumping density of spot B is varied; the theoretical investigation; and polariton condensation in the waveguide when a Gaussian-distributed large beam spot replaces the previous spot A configuration.

[43] H. Yoshida, Construction of higher order symplectic integrators, Phys. Lett. A **150**, 262 (1990).

[44] T. T. J. Shen and L. Wang, *Spectral Methods: Algorithms, Analysis and Applications* (Springer, Berlin, 2011).